

Supporting Information

Multianalyte On-chip Native Western Blotting

*Samuel Q. Tia,^a Mei He,^b Dohyun Kim^b and Amy E. Herr^{*ab}*

^a The UC Berkeley - UCSF Graduate Program in Bioengineering,
342 Stanley Hall, Berkeley, California 94720, USA.

^b Department of Bioengineering, University of California Berkeley,
342 Stanley Hall, Berkeley, California 94720, USA

*Corresponding Author: E-mail: aeh@berkeley.edu

Table of Contents

Figure S-1. Schematic diagram of multistep photolithographic gel fabrication

Figure S-2. Matrix illustration of positive and negative control experiments to assess size exclusion effects at blotting gel interfaces.

Figure S-3. Langmuir binding simulation schematic.

Table S-1. On-chip immunoblotting voltage control program for high voltage power supply

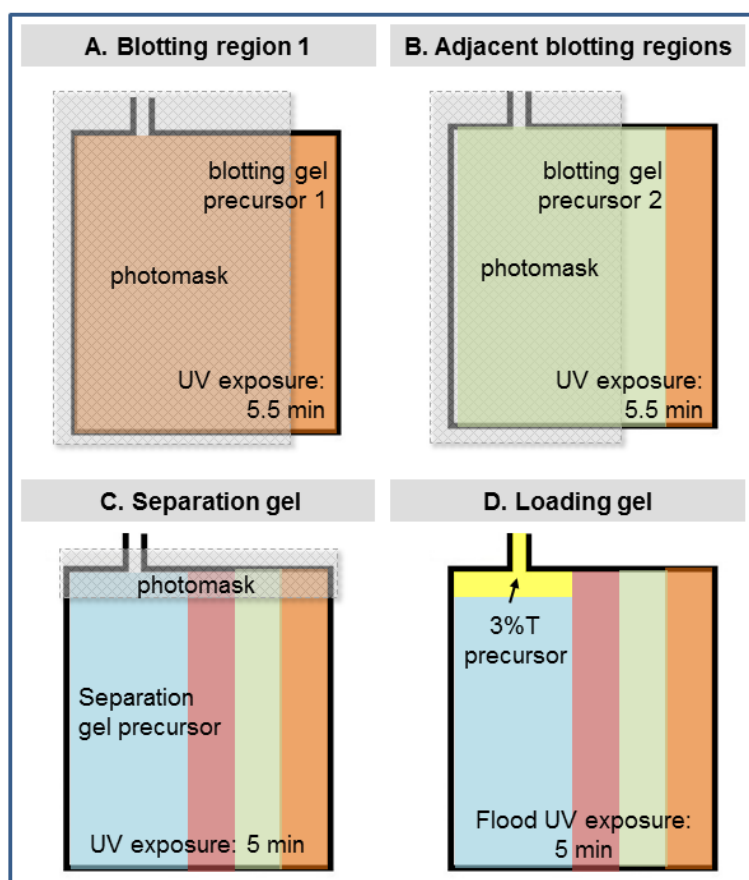


Figure S-1. Multi-step photolithography enables fabrication of multiple PA gel regions with varying physical and functional properties. The fabrication approach yields a device suitable for fully-automated, low sample loss, multi-analyte native Western blotting.

A Hamamatsu LightningCure LC5 UV light source (Hamamatsu City, Japan) with variable intensity control was used for photopatterning of the gels. The UV beam from the LC5 was directed along the light path of a Nikon Diaphot 200 (Tokyo, Japan) inverted microscope and up through a UV-transmission objective lens (UPLANS-APO 4x, Olympus, Melville, NY). The masked chip was then exposed to UV for 5 min and 30 s at 3.5 mW/cm^2 , as measured with a UV513AB Digital Light Meter (General Tools, New York NY). Unpolymerized material was evacuated and the precursor for the next blotting gel region was introduced to the central chamber by applying vacuum at the adjacent reservoirs. Visual inspection of the chip channels and chamber is performed before each photopolymerization step to avoid introduction of air bubbles. If observed, bubbles within the channels or chamber can be readily flushed out with a buffer solution via application of vacuum pressure and fresh PA gel precursor flushed in. When all requisite blotting regions were polymerized, the unpolymerized blotting gel precursor solution was evacuated from the central chamber and replaced with a 6% T PA separation gel solution.

The separation gel region was then masked to produce an interface near the top of the central chamber and exposed using the UV objective lens for 5 minutes at 3.5 mW/cm^2 . Finally, the lower density loading gel precursor was flushed through the uppermost loading channels and the entire chip was exposed to a filtered mercury lamp (UVP B100-AP, Upland, CA) with cooling fan. The final polymerization step required flood exposure for 5 minutes at 9 mW/cm^2 .

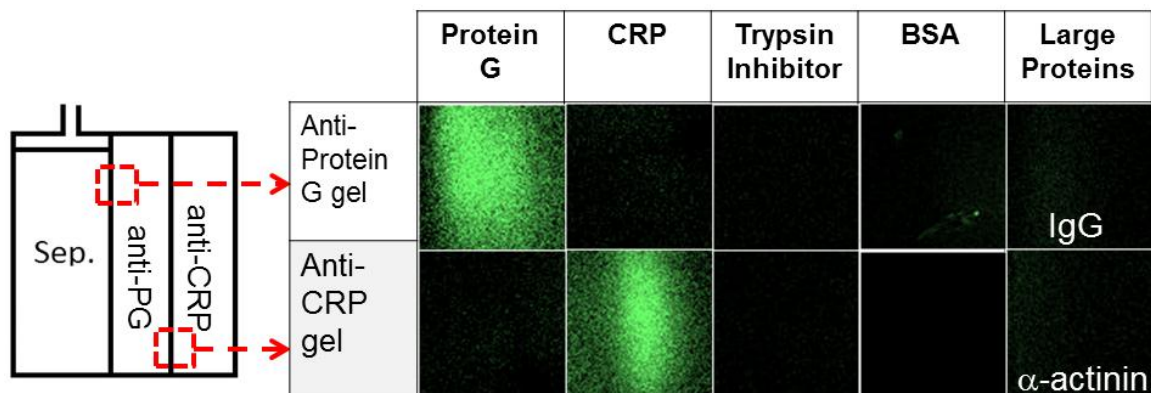


Figure S-2. Matrix displays post-transfer fluorescent microscope images taken at corresponding blotting regions within the device. Large fluorescently labeled non-target molecules are not retained at the blotting gel interface due to pore size exclusion or non-specific binding interactions. Positive controls show up as green fluorescence distribution upon corresponding blotting regions. Negative controls include high molecular weight species such as α -actinin and IgG (100 and 150 kDa, respectively).

To study size exclusion effects at the gel region interfaces, large analytes including BSA (66 kDa), α -actinin (100 kDa) and IgG (150 kDa) were assessed against anti-CRP and anti-protein G antibody-functionalized blotting regions. During sample transfer, fluorescence at the blotting interface and within the blotting regions was monitored. The large negative control proteins passed through the blotting region without exhibiting a decrease in electrophoretic mobility as they crossed from the separation gel into and out of the blotting region. BSA and α -actinin samples, assayed at 300 nM, displayed 5% and 4% residual signal at the separation gel to anti-PG and anti-CRP interfaces after each respective peak migrated across the blotting region.

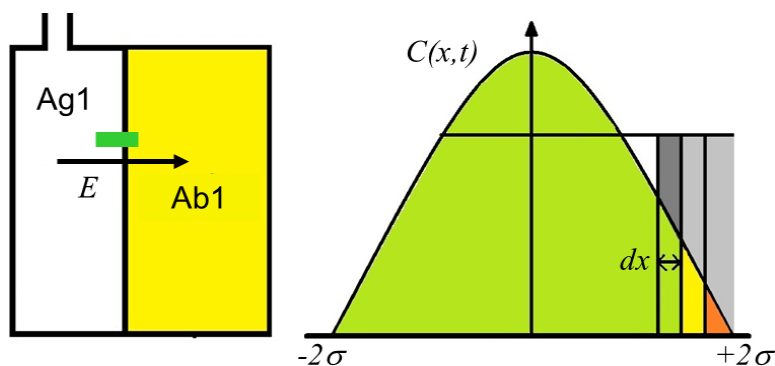


Figure S-3. The proposed model simulates Langmuir binding reactions between two sets of differential elements over a series of finite intervals. The migration speed determines a residence time step (Δt) wherein each target band element is co-localized or “incubated” with a matching gel element.

Table S-1. On-chip immunoblotting voltage control program (see Fig. 1 for electrode map).

The high voltage power supply employed here is custom fabricated hardware. Each of the 8 programmable electrodes is capable of current/voltage feedback control with a dynamic range of approximately 4000V and estimated $\pm 0.01 \mu\text{A}$ current and 1V voltage resolution.

Applied Voltage / Current	Electrode 1	Electrode 2	Electrode 3	Electrode 4	Electrode 5	Electrode 6	Electrode 7	Electrode 8
1. Sample loading	$0 \mu\text{A}$	-400 V	$-0.1 \mu\text{A}$	-200 V	$0 \mu\text{A}$	$0 \mu\text{A}$	$-0.05 \mu\text{A}$	$0 \mu\text{A}$
2. Injection / separation	-290 V	$0.1 \mu\text{A}$	-400 V	$0.1 \mu\text{A}$	-295 V	$0 \mu\text{A}$	-220 V	$0 \mu\text{A}$
3. Transfer & blotting	$0 \mu\text{A}$	$0.05 \mu\text{A}$	$0 \mu\text{A}$	$0.05 \mu\text{A}$	$0 \mu\text{A}$	-50 V	$0 \mu\text{A}$	-120 V